Genetic Characterization of Avian Influenza A(H5N6) Virus Clade 2.3.4.4, Russia, 2018

Ivan M. Susloparov, Natalia Goncharova, Natalia Kolosova, Alexey Danilenko, Vasiliy Marchenko, Galina Onkhonova, Vasiliy Evseenko, Elena Gavrilova, Rinat A. Maksutov, Alexander Ryzhikov

Author affiliation: State Research Center of Virology and Biotechnology Vector, Koltsovo, Russia

DOI: https://doi.org/10.3201/eid2512.190504

Timely identification of pandemic influenza threats depends on monitoring for highly pathogenic avian influenza viruses. We isolated highly pathogenic avian influenza A(H5N6) virus clade 2.3.4.4, genotype G1.1, in samples from a bird in southwest Russia. The virus has high homology to human H5N6 influenza strains isolated from southeast China.

Highly pathogenic avian influenza (HPAI) H5 virus continues to evolve and pose a threat to animals and humans. Since 2008, HPAI H5 viruses of clade 2.3.4.4 with various neuraminidase (NA) subtypes have become widespread throughout the world and have caused mass epizootics, including in Russia, where these viruses have been reported since 2014 (*1*). In 2013, H5N6 virus began circulating in China (*2*), and a case of human disease was recorded there in 2014. Since then, 23 cases of H5N6 infection in humans, including 7 fatalities, have been confirmed in China (*3*).

In October 2018, we collected cloacal swab samples from aquatic birds around the Volga River Basin in the Saratov region of Russia (51°26′11.7″N, 46°06′49.9″E). We isolated avian H5 influenza virus from 1 sample from a common gull (*Larus canus*) by using embryonic chicken eggs. We used whole-genome sequencing to extract the virus DNA and conducted a phylogenetic analysis against strains available in the GISAID EpiFlu database (http://www.gisaid.org). We submitted genetic data on the virus, A/common gull/Saratov/1676/2018, to the GISAID EpiFlu database (identification no. EPIISL336925).

Using H5 clade nomenclature designated by the World Health Organization/World Organisation for Animal Health/Food and Agriculture Organization H5 Evolution Working Group (*4*), our phylogenetic analysis showed that hemagglutinin (HA) gene of A/common gull/Saratov/1676/2018 clusters with HPAI viruses in clade 2.3.4.4 H5N6-H5/Major lineage. Our analyses also show this strain belongs to a new HA subgroup that includes human H5N6 viruses isolated in Guangxi and Guangdong Provinces, China, in 2018 (Appendix Figure 1, Table 1, https://wwwnc.cdc.gov/EID/article/25/12/19-0504-App1.pdf). This subgroup is not represented by existing candidate vaccine viruses (CVVs) (*5*,*6*).

The NA gene of A/common gull/Saratov/1676/2018 appears to originate from H6N6 viruses circulating in Asia during 2010–2011 (Appendix Figure 2) and contains the deletion from positions 59–69 in the stalk region. The polymerase basic (PB) 2 gene segment also appears to have originated from an H6 subtype (Appendix Figure 3). The internal gene segments PB1, polymerase (PA), nucleoprotein (NP), matrix (M), and nonstructural protein (NSP) appear to have evolved from HPAI H5 virus clade 2.3.2.1 (Appendix Figures 4–8). The 8-segment constellation leads us to classify this strain into a G1.1 genotype, as described by Bi et al. (*6*).

We conducted a comparative genomic analysis of A/common gull/Saratov/1676/2018 against H5N6 CVVs; the most pronounced differences were several amino acid substitutions associated with potential changes in antigenic properties. We also detected unique mutations in HA D54N, L115Q, L/Q138T, P141A, N183S, and N189D, including a combination of S121Y and I151T. We noted other mutations, including HA L129S, K/M/T140V (H5 numbering), and NA N86K (N6 numbering), which could be associated with antigenic drift.

A/common gull/Saratov/1676/2018 had an HA polybasic proteolytic cleavage site, PLRERRRKR/G, and showed highly pathogenic properties by killing chicken embryos within 48 hours. We also identified amino acid changes associated with increased virulence to mammals (*7*,*8*), including 9 mutations in the PB2 gene, 8 in the PB1 gene, 7 in the NSP gene, 3 in the M gene, 2 in the PA gene, 1 in the HA gene, and 1 in the NA gene, along with the 59–69 deletion, an 80–84 deletion in NS1, and an NS1 ESEV terminal motif. These changes also appear in most H5N6 CVVs (Appendix Table 2).

Comparative analysis of A/common gull/Saratov/1676/2018 against H5N6 CVVs revealed similarity in the presence of genetic elements associated with receptor binding properties. A/common gull/Saratov/1676/2018 and most CVVs had the motif QS(R)G at the receptor-binding site (nt 222–224), which is associated with an avian-like α2,3-SA receptor-binding preference (*6*). The amino acid changes in D94N, S133A, and T156A in the HA of A/common gull/Saratov/1676/2018 and most H5N6 CVVs are associated with increased binding of the virus to human-like α2,6-SA receptors (*7*). Our analysis suggests that A/common gull/Saratov/1676/2018 retains its avian status but has several mutations that potentially increase its affinity for α2,6-SA, which could indicate an affinity for both avian- and human-type receptors.

We evaluated the phenotypic properties of the virions by kinetics measurement with surface plasmon resonance to assess their ability to bind to receptor analogs α2,3-SA

and α2,6-SA (*9*). The equilibrium dissociation constant for 3′-Sialyl-N-acetyllactosamine is 12.2 (SD ± 0.7 nmol/L) and for 6′-Sialyl-N-acetyllactosamine is 43.3 (SD ± 2.8 nmol/L) (Appendix). These values show that A/common gull/Saratov/1676/2018 has prevalent affinity for the avian-like receptor with lower, but increased, affinity for the human-like receptor, compared with H5N1 strain A/rook/Chany/32/2015 clade 2.3.2.1.C.

Analysis of homology of A/common gull/Saratov/1676/2018 with H5N6 strains available from GISAID showed that all 8 gene segments clustered with human H5N6 strains isolated in southeast China in 2018. We noted 99% homology with human strain A/Guangxi/32797/2018 for all genes, a genetic similarity that raises the question of which pathway led to the spread of the virus. We believe A/common gull/Saratov/1676/2018 was transferred to eastern Russia through northeast Siberia, where HPAI H5N8 clade 2.3.4.4.A was detected in 2018 (*10*), the same pathway through which H5N8 virus was transferred from Southeast Asia to Europe. These viral pathogens could be spread by migratory birds over long distances along flyways from southern China to southwestern Russia during a migration season. Our study indicates that emerging H5N6 viruses are a potential threat to public health.

Acknowledgments

We are grateful to GISAID's EpiFlu Database (http://www.gisaid.org) and to the authors who provided sequence information.

This research was supported by State Assignment no. 13/19 FBRI SRC VB VECTOR Rospotrebnadzor.

About the Author

Dr. Susloparov is a senior researcher at the Zoonosis Infections and Influenza Department, State Research Center of Virology and Biotechnology Vector, Koltsovo, Russia. His research interests include the molecular genetics, epidemiology, and host–pathogen interaction of avian influenza viruses.

References

1. Marchenko V, Goncharova N, Susloparov I, Kolosova N, Gudymo A, Svyatchenko S, et al. Isolation and characterization of H5Nx highly pathogenic avian influenza viruses of clade 2.3.4.4 in Russia. Virology. 2018;525:216–23. https://doi.org/10.1016/j.virol.2018.09.024
2. Bi Y, Liu H, Xiong C, Di Liu, Shi W, Li M, et al. Novel avian influenza A (H5N6) viruses isolated in migratory waterfowl before the first human case reported in China, 2014. Sci Rep. 2016;6:29888. https://doi.org/10.1038/srep29888
3. World Health Organization. Regional Office for the Western Pacific. Avian Influenza Weekly Update Number 671. Geneva: the Organization; 2019 Jan 11 [cited 2019 Jan 11]. https://apps.who.int/iris/bitstream/handle/10665/279855/AI-20190111.pdf
4. Smith GJ, Donis RO; World Health Organization/World Organisation for Animal Health/Food and Agriculture Organization (WHO/OIE/FAO) H5 Evolution Working Group. Nomenclature updates resulting from the evolution of avian influenza A(H5) virus clades 2.1.3.2a, 2.2.1, and 2.3.4 during 2013–2014. Influenza Other Respir Viruses. 2015;9:271–6. https://doi.org/10.1111/irv.12324
5. World Health Organization. Antigenic and genetic characteristics of zoonotic influenza viruses and development of candidate vaccine viruses for pandemic preparedness. Geneva: the Organization; February 2019 [cited 2019 Feb 21]. https://www.who.int/influenza/vaccines/virus/201902_zoonotic_vaccinevirusupdate.pdf
6. Bi Y, Chen Q, Wang Q, Chen J, Jin T, Wong G, et al. Genesis, evolution, and prevalence of H5N6 avian influenza viruses in China. Cell Host Microbe. 2016;20:810–21. https://doi.org/10.1016/j.chom.2016.10.022
7. Guo F, Luo T, Pu Z, Xiang D, Shen X, Irwin DM, et al. Increasing the potential ability of human infections in H5N6 avian influenza A viruses. J Infect. 2018;77:349–56. https://doi.org/10.1016/j.jinf.2018.07.015
8. Yang L, Zhu W, Li X, Bo H, Zhang Y, Zou S, et al. Genesis and dissemination of highly pathogenic H5N6 avian influenza viruses. J Virol. 2017;91:e02199–16. https://doi.org/10.1128/JVI.02199-16
9. Meng B, Marriott AC, Dimmock NJ. The receptor preference of influenza viruses. Influenza Other Respir Viruses. 2010;4:147–53. https://doi.org/10.1111/j.1750-2659.2010.00130.x
10. Verhagen JH, Herfst S, Fouchier RA. Infectious disease. How a virus travels the world. Science. 2015;347:616–7. https://doi.org/10.1126/science.aaa6724

Address for correspondence: Ivan M. Susloparov, State Research Center of Virology and Biotechnology Vector, 630559, Koltsovo, Novosibirsk Region, Russia; email: imsous@vector.nsc.ru

Human Parasitism by *Amblyomma parkeri* Ticks Infected with *Candidatus* Rickettsia paranaensis, Brazil

Ana Beatriz P. Borsoi, Karla Bitencourth, Stefan V. de Oliveira, Marinete Amorim, Gilberto S. Gazêta

Author affiliations: Instituto Oswaldo Cruz, Rio de Janeiro, Brazil (A.B.P. Borsoi, K. Bitencourth, M. Amorim, G.S. Gazêta); Universidade Federal de Uberlândia, Uberlândia, Brazil (S.V. de Oliveira); Ministério da Saúde do Brasil, Brasília, Brazil (S.V. de Oliveira)

DOI: https://doi.org/10.3201/eid2512.1909819-0988

Article DOI: https://doi.org/10.3201/eid2512.190504

Genetic Characterization of Avian Influenza A(H5N6) Virus Clade 2.3.4.4, Russia, 2018

Appendix

Measurement of Equilibrium Dissociation Constants

To determine receptor preference, we measured binding kinetics of virions to receptor analogs by surface plasma resonance on a ProteOn XPR36 (Bio-Rad, https://www.bio-rad.com) with a NeutrAvidin chip (Bio-Rad) and 3′-Sialyl-N-acetyllactosamine and 6′-Sialyl-N-acetyllactosamine biotinylated receptor analogs (Dextra, https://www.dextrauk.com). We immobilized α2–3 and α2–6 glycans on the NLC chip in sodium phosphate buffer (pH 7.4) at a concentration of 100 μg/mL. We injected 5 dilutions of purified virus sample in the same buffer at a flow rate of 70 μL/min with 350 seconds contact time for association. Dissociation lasted 600 seconds at the same flow rate. We added oseltamivir (20 nmol/L) to inhibit neuraminidase. We analyzed data with the ProteOn Manager (Bio-Rad) software using Langmuir kinetics calculations model (Appendix Figure 9). We calculated equilibrium dissociation constants (K_D) as ratio of dissociation and association constants: $K_D = k_d/k_a$. We used 3 independent surface plasma resonance runs to verify the equilibrium dissociation constants.

K_D for 3′SLN and 6′SLN of A/common gull/Saratov/1676/2018

K_D for 3′SLN = 12.2 ± 0.7 nmol/L

K_D for 6′SLN = 43.3 ± 2.8 nmol/L

K_D for 3′SLN and 6′SLN of A/rook/Chany/32/2015

K_D for 3′SLN = 0.2 ± 0.02 μmol/L

K_D for 6′SLN = 6.3 ± 0.1 μmol/L

The data confirms preferential binding of both strains to α2,3-SA.

Appendix Table 1. Comparison of gene segments of avian influenza A(H5N6) virus clade 2.3.4.4 isolated in Russia, 2018 with human influenza A H5N6 viruses*

Gene segment	GISAID no.	Guangxi/32797/ 2018	Guangxi/31906/ 2018	Guangdong/ 18SF020/2018	Guangxi/13486/2017	Jiangsu/32888/2018
HA	EPI1355418	1,763/1,773 (99)	1,753/1,772 (98)	1,753/1,774 (98)	1,744/1,774 (98)	1,723/1,775 (97)
NA	EPI1355420	1,430/1,432 (99)	1,416/1,432 (98)	1,411/1,432 (98)	1,418/1,432 (99)	1,378/1,435 (96)
PB2	EPI1355415	2,330/2,335 (99)	2,324/2,341 (99)	2,303/2,326 (99)	2,303/2,326 (99)	2,283/2,326 (98)
PB1	EPI1355416	2,290/2,301 (99)	2,310/2,341 (98)	2,237/2,274 (98)	2,256/2,274 (99)	2,300/2,331 (98)
PA	EPI1355417	2,225/2,233 (99)	2,209/2,233 (98)	2,123/2,151 (98)	2,132/2,151 (99)	2,017/2,214 (91)
NP	EPI1355419	1,540/1,543 (99)	1,548/1,565 (98)	1,550/1,565 (99)	1,551/1,565 (99)	1,550/1,565 (99)
M	EPI1355421	1,022/1,027 (99)	1,018/1,027 (99)	1,024/1,028 (99)	1,003/1,012 (99)	1,018/1,027 (99)
NSP	EPI1355422	868/870 (99)	865/875 (98)	870/875 (99)	872/875 (99)	871/876 (99)

*Avian influenza A(H5N6) isolated in this study, A/common gull/Saratov/1676/2018 in Global Initiative on Sharing All Influenza Data database. Values for nucleic sequence homology of each gene segment expressed as gene segments of A/common gull/Saratov/1676/2018 versus gene segments of human A(H5N6). Values in parentheses represent % identity. GSAID, Global Initiative on Sharing All Influenza Data HA, hemagglutinin; M, matrix; NA, neuraminidase; NP, nucleoprotein; NSP, nonstructural protein; PA, polymerase; PB1, polymerase basic 1; PB2, polymerase basic 2.

Appendix Table 2. Amino acid changes in proteins of avian influenza A(H5N6) compared with the closest homologue and H5N6 candidate vaccine viruses*

	Human H5N6 virus strains				Avian H5N6 virus strains			
Gene	A/Hubei/ 29578/ 2016†	A/Fujian-Sanyuan/ 21099/ 2017†	A/Sichuan/ 26221/ 2014†	A/Guangxi/ 32797/ 2018†	A/chicken/ Vietnam/ NCVD-15A59/2015†	A/duck/ Hyogo/ 1/2016†	A/common gull/ Saratov/ 1676/2018	Phenotypic characteristics
HA (H5 no.)								
D54N	D	D	D	N	D	D	N	Creates a potential N-glycosylation site
D94N	N	S	N	N	N	N	N	Increased virus binding to α2–6
L115Q	L	L	L	Q	L	L	Q	Antigenic drift
S121Y	S	S	S	S	S	S	Y	Together with I151T antigenic drift
S123P	P	P	T	S	P	P	S	Increased virus binding to α2–6
126 Del	Del	E	E	Del	E	E	Del	Creates a potential N-glycosylation site
L129S	S	L	L	S	L	Del	S	Position associated with antigenic drift
S133A	A	A	A	A	A	A	A	Increased virus binding to α2–6
L/Q138T	L	Q	Q	T	Q	Q	T	Position associated with antigenic drift
K/M/T140V	K	T	T	V	M	V	V	Position associated with antigenic drift
P141A	P	P	P	A	P	P	A	Antigenic drift
I151T	T	I	I	T	T	T	T	With S121Y, antigenic drift; with 129Del, host specificity shift
T156A	A	A	A	A	A	A	A	Increased virus binding to α2–6
N183S	N	N	N	S	N	N	S	Position associated with antigenic drift, host specificity shift
T188A	T	T	T	A	T	T	A	Host specificity shift
N189D	N	N	N	D	N	N	D	Antigenic drift
220–224	NGQSG	NGQRG	NGQRG	NGQHG	NGQRG	NGQQG	NGQRG	222–224 QS(R)G avian-like α2–3 receptor-binding preference
A263T	T	T	T	T	T	T	T	Increased virulence in mammals
Cleavage peptides	RERRRKR	REKRRKR	REKRRKR	RERRRKR	RERRRKR	RERRRKR	RERRRKR	Highly pathogenic avian influenza
NA (N6 no.)								
59–69 Del	yes	yes	no	yes	yes	yes	yes	Enhanced virulence in mice
N86K	N	K	N	K	N	K	K	Removes a potential N-glycosylation site
T223I	I	I	I	I	I	I	I	Increased virulence in mammals
PB2								
T63I	I	I	I	I	I	I	I	Increased virulence in mammals
L89V	V	V	V	V	V	V	V	Leu89Val, Gly309Asp, Thr339Lys, Arg477Gly, Ile495Val, Lys627Glu, Ala676Thr; enhanced polymerase activity and increased virulence in mice
G309D	D	D	D	D	D	D	D	Leu89Val, Gly309Asp, Thr339Lys, Arg477Gly, Ile495Val, Lys627Glu, Ala676Thr; enhanced polymerase activity and increased virulence in mice
T339K	K	K	M	K	T	K	K	Leu89Val, Gly309Asp, Thr339Lys, Arg477Gly,

Gene	Human H5N6 virus strains				Avian H5N6 virus strains			Phenotypic characteristics
	A/Hubei/ 29578/ 2016†	A/Fujian-Sanyuan/ 21099/ 2017†	A/Sichuan/ 26221/ 2014†	A/Guangxi/ 32797/ 2018†	A/chicken/ Vietnam/ NCVD-15A59/2015†	A/duck/ Hyogo/ 1/2016†	A/common gull/ Saratov/ 1676/2018	
								Ile495Val, Lys627Glu, Ala676Thr; enhanced polymerase activity and increased virulence in mice
Q368R	R	R	Q	R	Q	R	R	Increased virulence in mammals
H447Q	Q	Q	Q	Q	Q	Q	Q	Increased virulence in mammals
R477G	G	G	G	G	G	G	G	Leu89Val, Gly309Asp, Thr339Lys, Arg477Gly, Ile495Val, Lys627Glu, Ala676Thr; enhanced polymerase activity and increased virulence in mice
I495V	V	V	V	V	V	V	V	Leu89Val, Gly309Asp, Thr339Lys, Arg477Gly, Ile495Val, Lys627Glu, Ala676Thr; enhanced polymerase activity and increased virulence in mice
A/T588V	A	A	T	V	T	V	V	Host specificity shift
K627E	E	E	E	K	E	E	E	Enhanced polymerase activity and increased virulence in mice, adaptation to mammals
A661S	A	A	A	S	A	S	S	Host specificity shift
A676T	M	T	T	T	T	T	T	Leu89Val, Gly309Asp, Thr339Lys, Arg477Gly, Ile495Val, Lys627Glu, Ala676Thr; enhanced polymerase activity and increased virulence in mice
PB1								
A3V	V	V	V	V	V	V	V	Increased virulence in mammals
L13P	P	P	P	P	P	P	P	Increased virulence in mammals
R207K	K	K	K	K	K	K	K	Increased virulence in mammals
K328N	N	N	N	N	N	N	N	Increased virulence in mammals
I368V	V	I	I	I	I	I	I	Increased transmission in ferrets
S375N	N	N	N	N	N	N	N	Increased virulence in mammals
H436Y	Y	Y	Y	Y	Y	Y	Y	Increased virulence in mammals
L473V	V	V	V	V	V	V	V	Increased virulence in mammals
M677T	T	T	T	T	T	T	T	Increased virulence in mammals
PA								
V100A	I	V	V	V	V	V	V	Species associated signature position
G225S	S	S	G	S	S	S	S	Host specificity shift
H266R	R	R	R	R	R	R	R	Increased virulence in mammals
K356R	R	K	K	K	K	K	K	Species associated signature position
S409N	N	S	S	S	S	S	S	Species associated signature position
S/A515T	T	T	T	T	T	T	T	Increased virulence in mammals
NP								
I33V	V	V	I	V	V	V	V	Host specificity shift
M1								
V15I	I	V	I	I	I	I	I	Increased virulence in mammals
N30D	D	D	D	D	D	D	D	Increased virulence in mice
T215A	A	A	A	A	A	A	A	Increased virulence in mice
M2								
S31N	N	S	S	S	S	S	S	Resistance to adamantine
S89G	G	G	S	G	G	G	G	Host specificity shift
NSP1								
P42S	S	S	S	S	S	S	S	Increased virulence in mice
80–84 del	No	No	Yes	Yes	Yes	Yes	Yes	Increased virulence in mice
D92E‡	D	D	E	E	E	E	E	Increased virulence in mammals

Gene	Human H5N6 virus strains				Avian H5N6 virus strains			Phenotypic characteristics
	A/Hubei/ 29578/ 2016†	A/Fujian-Sanyuan/ 21099/ 2017†	A/Sichuan/ 26221/ 2014†	A/Guangxi/ 32797/ 2018†	A/chicken/ Vietnam/ NCVD-15A59/2015†	A/duck/ Hyogo/ 1/2016†	A/common gull/ Saratov/ 1676/2018	
L98F§	L	F	F	F	F	F	F	Increased virulence in mice
I101M§	I	M	M	M	M	M	M	Increased virulence in mice
V149A¶	A	A	A	A	A	A	A	Increased virulence in mammals
N200S§	S	S	S	S	S	S	S	Asn200Ser, when coupled with NS2 Thr47Ala; increased virulence in mammals
Terminal motif ESEV	Truncated	GSEV	ESEV	ESEV	ESEV	ESEV	ESEV	Increased virulence in mice
NSP2								
T47A	A	A	A	A	A	A	A	Thr47Ala (when coupled with NS1 Asn200Ser) Increased virulence in mammals

*Avian influenza A(H5N6) from this study, A/common gull/Saratov/1676/2018 in Global Initiative on Sharing All Influenza Data database. HA, hemagglutinin; M1, matrix 1; M2, matrix 2; NA, neuraminidase; NP, nucleoprotein; NSP1, nonstructural protein 1; NSP2, nonstructural protein 2;PA, polymerase; PB1, polymerase basic 1; PB2, polymerase basic 2.
†Candidate vaccine virus.
‡87 if the deletion is not counted.
§Deletion not counted.
¶144 if deletion not counted.

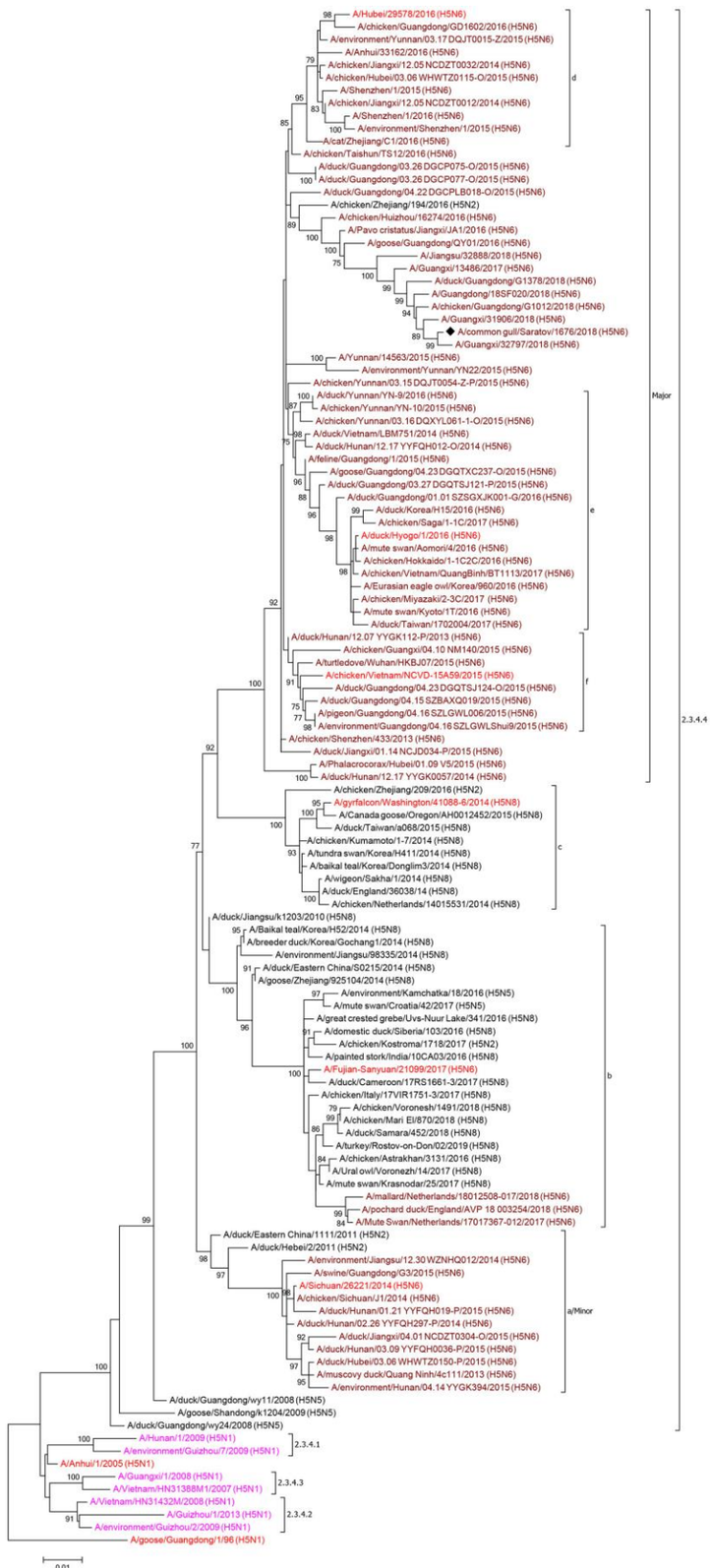

Appendix Figure 1. Phylogenetic analysis of the hemagglutinin (HA) gene segment of A/common gull/Saratov/1676/2018 (H5N6) isolated from a common gull (*Larus canus*) in the Saratov Region of Russia, 2018. Phylogenetic analysis was performed by using MEGA version 6.0 (http://www.megasoftware.net) and the maximum likelihood method with 500 bootstrap replications. Genetic clusters of avian influenza viruses are annotated by brackets. Numbers near the branches indicate bootstrap value >70%. Influenza virus sequences were deposited in Global Initiative on Sharing All Influenza Data (GISAID; https://platform.gisaid.org/epi3) under identification no. EPI1355418. Sequence data from the Influenza Research Database (IRD; https://www.fludb.org) and GenBank (https://www.ncbi.nlm.nih.gov/genbank) were used for comparison. Black diamond indicates isolate from this study. Red text indicates candidate vaccine viruses. Blue text indicates H9N2/H7N9 sequences; green text indicates H6 subtypes; pink text indicates H5N1 subtypes; brown text indicates H5N6 subtypes. Scale bar indicates nucleotide substitutions per site.

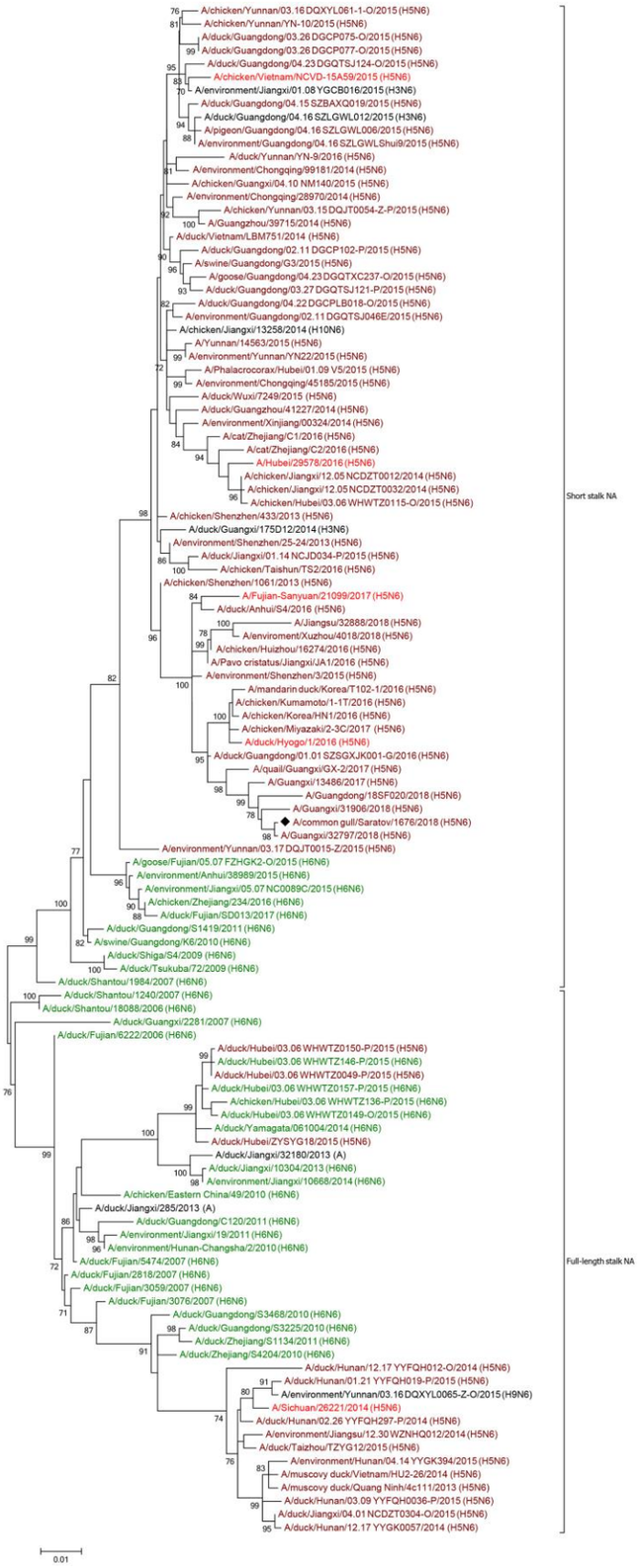

Appendix Figure 2. Phylogenetic analysis of the neuraminidase (NA) gene segment of A/common gull/Saratov/1676/2018 (H5N6) isolated from a common gull (*Larus canus*) in the Saratov Region of Russia, 2018. Phylogenetic analysis was performed by using MEGA version 6.0 (http://www.megasoftware.net) and the maximum likelihood method with 500 bootstrap replications. Genetic clusters of avian influenza viruses are annotated by brackets. Numbers near the branches indicate bootstrap value >70%. Influenza virus sequences were deposited in Global Initiative on Sharing All Influenza Data (GISAID; https://platform.gisaid.org/epi3) under identification no. EPI1355418. Sequence data from the Influenza Research Database (IRD; https://www.fludb.org) and GenBank (https://www.ncbi.nlm.nih.gov/genbank) were used for comparison. Black diamond indicates isolate from this study. Red text indicates candidate vaccine viruses. Blue text indicates H9N2/H7N9 sequences; green text indicates H6 subtypes; pink text indicates H5N1 subtypes; brown text indicates H5N6 subtypes. Scale bar indicates nucleotide substitutions per site.

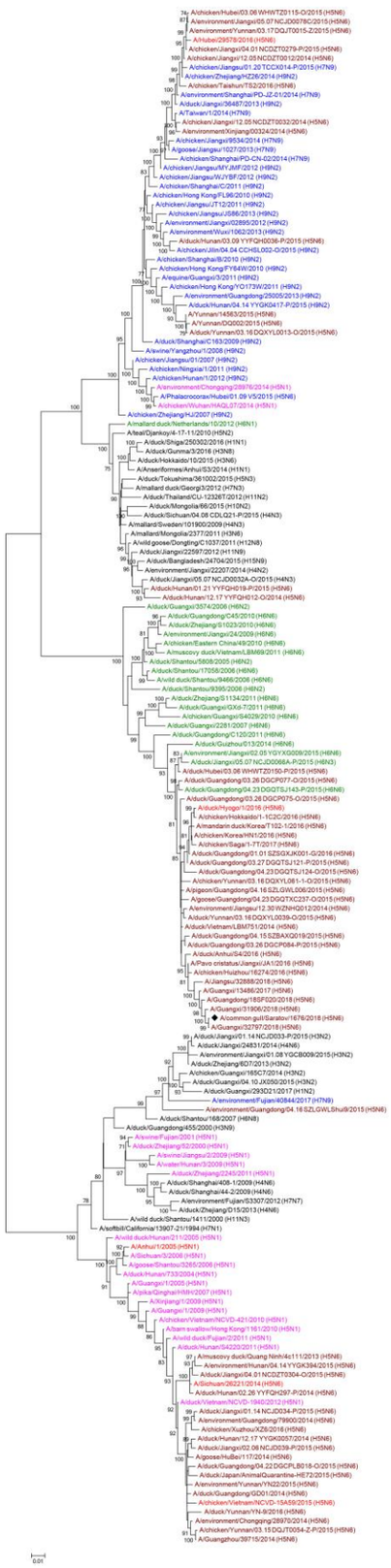

Appendix Figure 3. Phylogenetic analysis of the polymerase basic protein 2 (PB2) gene segment of A/common gull/Saratov/1676/2018 (H5N6) isolated from a common gull (*Larus canus*) in the Saratov Region of Russia, 2018. Phylogenetic analysis was performed by using MEGA version 6.0 (http://www.megasoftware.net) and the maximum likelihood method with 500 bootstrap replications. Numbers near the branches indicate bootstrap value >70%. Influenza virus sequences were deposited in Global Initiative on Sharing All Influenza Data (GISAID; https://platform.gisaid.org/epi3 under identification no. EPI1355418. Sequence data from the Influenza Research Database (IRD; https://www.fludb.org) and GenBank (https://www.ncbi.nlm.nih.gov/genbank) were used for comparison. Black diamond indicates isolate from this study. Red text indicates candidate vaccine viruses. Blue text indicates H9N2/H7N9 sequences; green text indicates H6 subtypes; pink text indicates H5N1 subtypes; brown text indicates H5N6 subtypes. Scale bar indicates nucleotide substitutions per site.

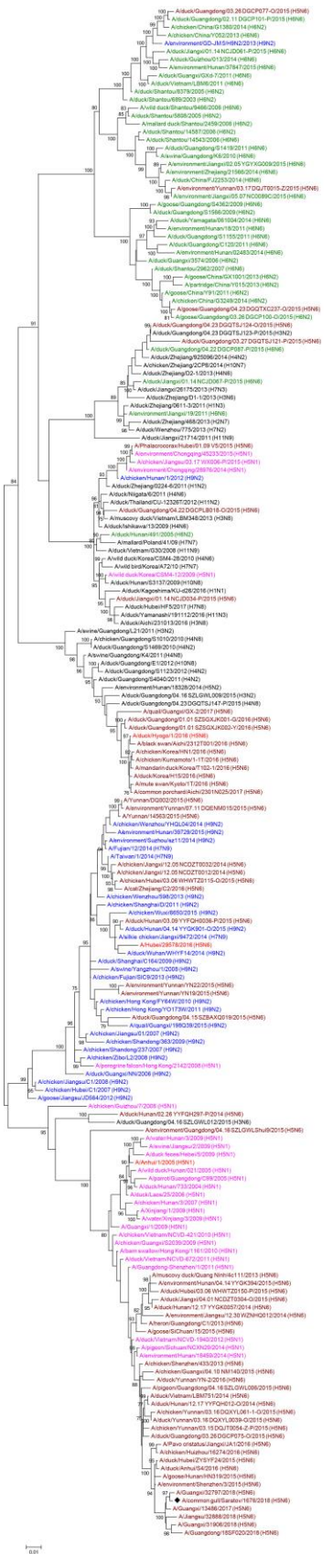

Appendix Figure 4. Phylogenetic analysis of the polymerase basic protein 1 (PB1) gene segment of A/common gull/Saratov/1676/2018 (H5N6) isolated from a common gull (*Larus canus*) in the Saratov Region of Russia, 2018. Phylogenetic analysis was performed by using MEGA version 6.0 (http://www.megasoftware.net) and the maximum likelihood method with 500 bootstrap replications. Numbers near the branches indicate bootstrap value >70%. Influenza virus sequences were deposited in Global Initiative on Sharing All Influenza Data (GISAID; https://platform.gisaid.org/epi3) under identification no. EPI1355418. Sequence data from the Influenza Research Database (IRD; https://www.fludb.org) and GenBank (https://www.ncbi.nlm.nih.gov/genbank) were used for comparison. Black diamond indicates isolate from this study. Red text indicates candidate vaccine viruses. Blue text indicates H9N2/H7N9 sequences; green text indicates H6 subtypes; pink text indicates H5N1 subtypes; brown text indicates H5N6 subtypes. Scale bar indicates nucleotide substitutions per site.

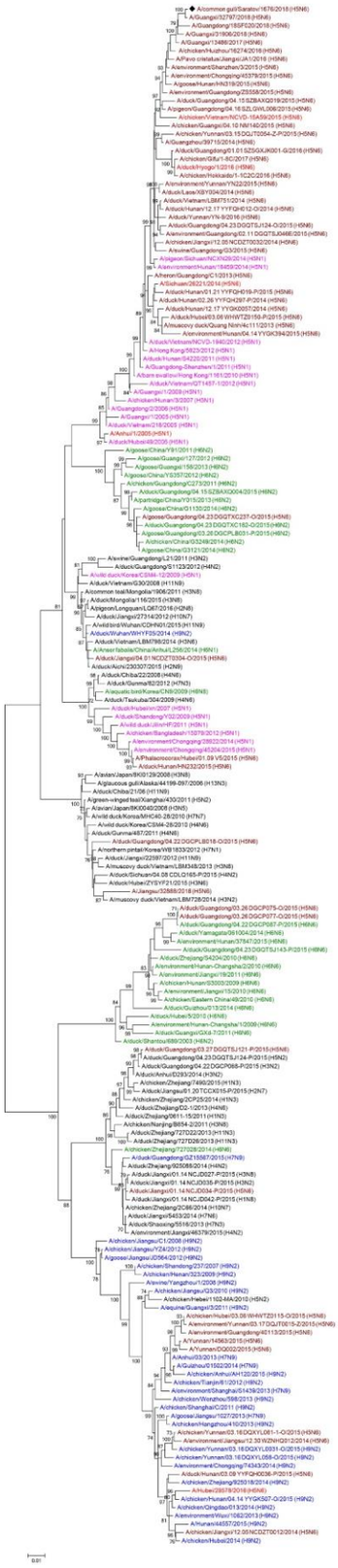

Appendix Figure 5. Phylogenetic analysis of the polymerase acidic (PA) gene segment of A/common gull/Saratov/1676/2018 (H5N6) isolated from a common gull (*Larus canus*) in the Saratov Region of Russia, 2018. Phylogenetic analysis was performed by using MEGA version 6.0 (http://www.megasoftware.net) and the maximum likelihood method with 500 bootstrap replications. Numbers near the branches indicate bootstrap value >70%. Influenza virus sequences were deposited in Global Initiative on Sharing All Influenza Data (GISAID; https://platform.gisaid.org/epi3) under identification no. EPI1355418. Sequence data from the Influenza Research Database (IRD; https://www.fludb.org) and GenBank (https://www.ncbi.nlm.nih.gov/genbank) were used for comparison. Black diamond indicates isolate from this study. Red text indicates candidate vaccine viruses. Blue text indicates H9N2/H7N9 sequences; green text indicates H6 subtypes; pink text indicates H5N1 subtypes; brown text indicates H5N6 subtypes. Scale bar indicates nucleotide substitutions per site.

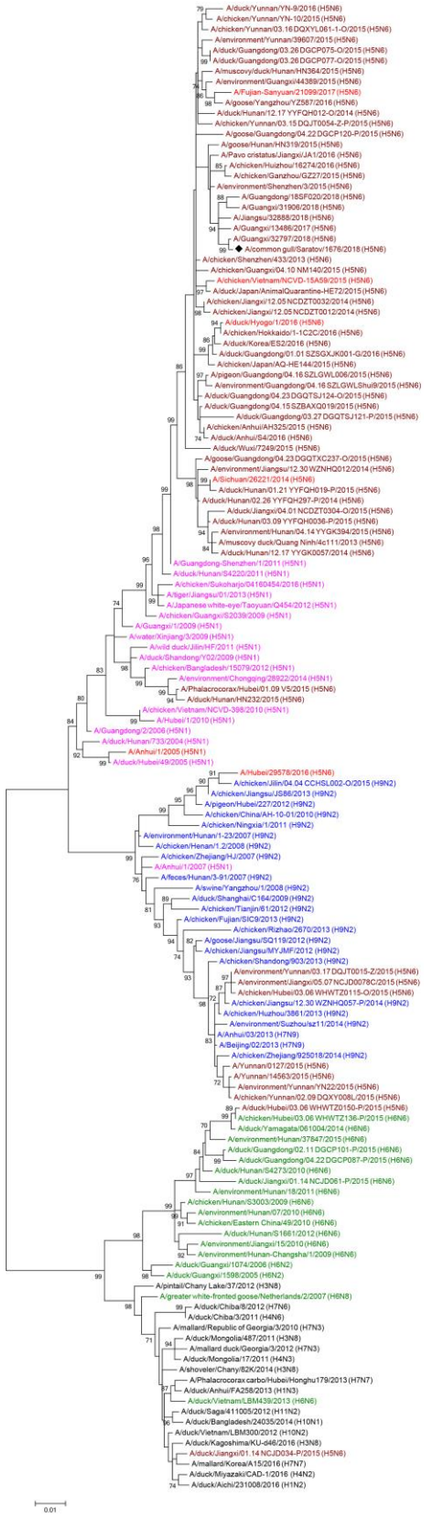

Appendix Figure 6. Phylogenetic analysis of the nucleoprotein (NP) gene segment of A/common gull/Saratov/1676/2018 (H5N6) isolated from a common gull (*Larus canus*) in the Saratov Region of Russia, 2018. Phylogenetic analysis was performed by using MEGA version 6.0 (http://www.megasoftware.net) and the maximum likelihood method with 500 bootstrap replications. Numbers near the branches indicate bootstrap value >70%. Influenza virus sequences were deposited in Global Initiative on Sharing All Influenza Data (GISAID; https://platform.gisaid.org/epi3) under identification no. EPI1355418. Sequence data from the Influenza Research Database (IRD; https://www.fludb.org) and GenBank (https://www.ncbi.nlm.nih.gov/genbank) were used for comparison. Black diamond indicates isolate from this study. Red text indicates candidate vaccine viruses. Blue text indicates H9N2/H7N9 sequences; green text indicates H6 subtypes; pink text indicates H5N1 subtypes; brown text indicates H5N6 subtypes. Scale bar indicates nucleotide substitutions per site.

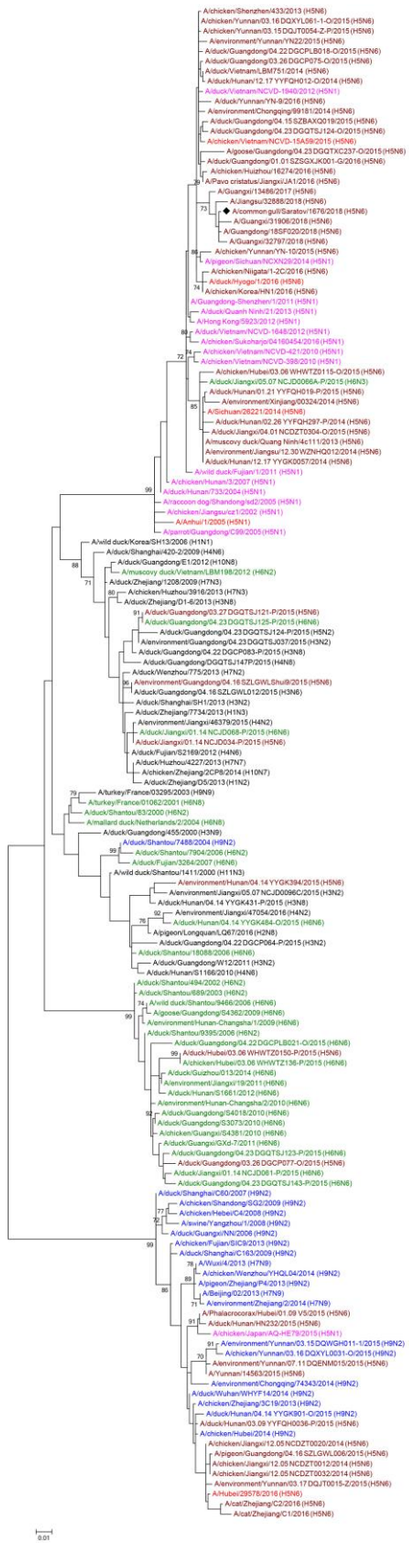

Appendix Figure 7. Phylogenetic analysis of the matrix (M) gene segment of A/common gull/Saratov/1676/2018 (H5N6) isolated from a common gull (*Larus canus*) in the Saratov Region of Russia, 2018. Phylogenetic analysis was performed by using MEGA version 6.0 (http://www.megasoftware.net) and the maximum likelihood method with 500 bootstrap replications. Numbers near the branches indicate bootstrap value >70%. Influenza virus sequences were deposited in Global Initiative on Sharing All Influenza Data (GISAID; https://platform.gisaid.org/epi3) under identification no. EPI1355418. Sequence data from the Influenza Research Database (IRD; https://www.fludb.org) and GenBank (https://www.ncbi.nlm.nih.gov/genbank) were used for comparison. Black diamond indicates isolate from this study. Red text indicates candidate vaccine viruses. Blue text indicates H9N2/H7N9 sequences; green text indicates H6 subtypes; pink text indicates H5N1 subtypes; brown text indicates H5N6 subtypes. Scale bar indicates nucleotide substitutions per site.

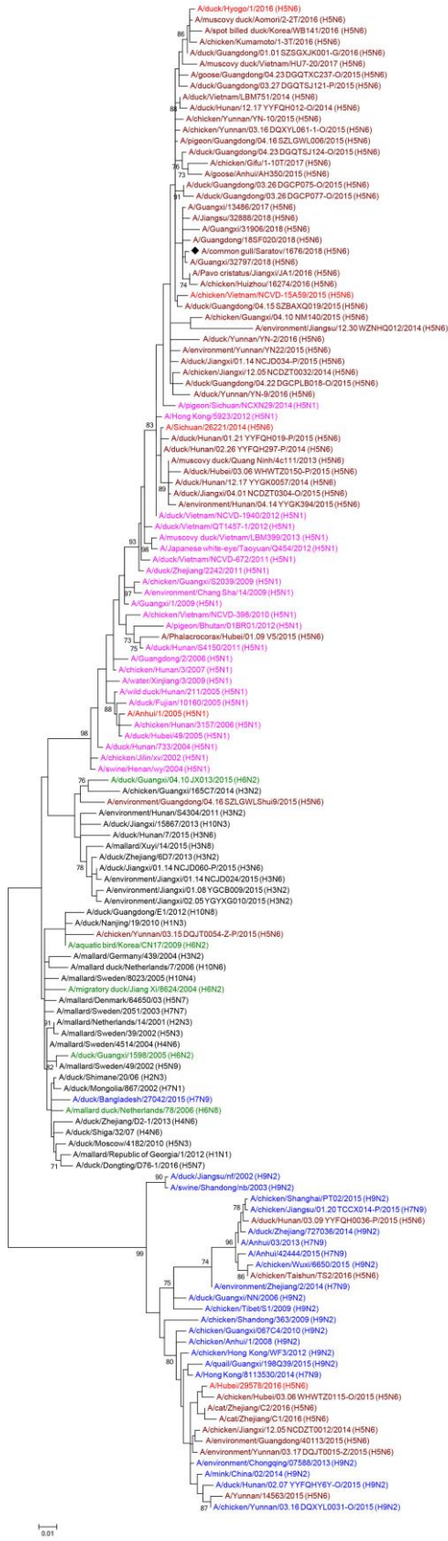

Appendix Figure 8. Phylogenetic analysis of the nonstructural protein (NSP) gene segment of A/common gull/Saratov/1676/2018 (H5N6) isolated from a common gull (*Larus canus*) in the Saratov Region of Russia, 2018. Phylogenetic analysis was performed by using MEGA version 6.0 (http://www.megasoftware.net) and the maximum likelihood method with 500 bootstrap replications. Numbers near the branches indicate bootstrap value >70%. Influenza virus sequences were deposited in Global Initiative on Sharing All Influenza Data (GISAID; https://platform.gisaid.org/epi3) under identification no. EPI1355418. Sequence data from the Influenza Research Database (IRD; https://www.fludb.org) and GenBank (https://www.ncbi.nlm.nih.gov/genbank) were used for comparison. Black diamond indicates isolate from this study. Red text indicates candidate vaccine viruses. Blue text indicates H9N2/H7N9 sequences; green text indicates H6 subtypes; pink text indicates H5N1 subtypes; brown text indicates H5N6 subtypes. Scale bar indicates nucleotide substitutions per site.

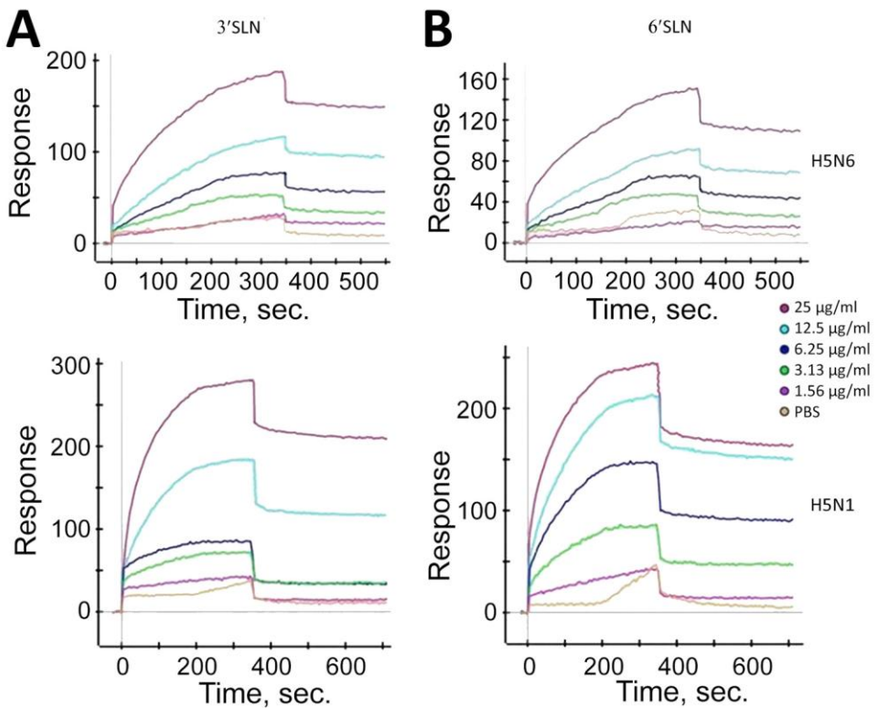

Appendix Figure 9. Surface plasma resonance sensorgrams for interaction of A/common gull/Saratov/1676/2018 (H5N6) and A/rook/Chany/32/2015 (H5N1) using receptor analogs for A) 3′SLN and B) 6′SLN after injection of viruses at the indicated concentrations. We used phosphate-buffered saline as a reference, which indicated specific binding between the virus and glycans. PBS, phosphate-buffered saline.